THE JOURNAL OF BIOLOGICAL CHEMISTRY
Vol. 270, No. 44, Issue of November 3, pp. 26159–26167, 1995

Printed in U.S.A.

Mycobacterium tuberculosis Chaperonin 10 Forms Stable Tetrameric and Heptameric Structures

IMPLICATIONS FOR ITS DIVERSE BIOLOGICAL ACTIVITIES*

(Received for publication, April 10, 1995, and in revised form, July 31, 1995)

Gianluca Fossati, Pierluigi Lucietto, Paola Giuliani, Anthony R. Coates‡, Steve Harding§, Helmut Cölfen§¶, Giuseppe Legname, Edith Chan, Andrea Zaliani, and Paolo Mascagni‖

From the Department of Chemistry, Italfarmaco Research Centre, Via Lavoratori 54, Cinisello Balsamo, 20092 Milan, Italy, the ‡Department of Medical Microbiology, St. George's Hospital Medical School, London SW17 0RE, United Kingdom, and the §Department of Applied Biochemistry and Food Science, University of Nottingham, Nottingham LE12 5RD, United Kingdom

The chaperonin activity of sequence-related chaperonin 10 proteins requires their aggregation into heptameric structures. We describe size-exclusion chromatography and ultracentrifugation studies that reveal that while *Escherichia coli* chaperonin 10 exists as a heptamer, the *Mycobacterium tuberculosis* chaperonin 10 is tetrameric in dilute solutions and in whole *M. tuberculosis* lysate. At high protein concentration and in the presence of saturating amounts of divalent ions, the protein is heptameric. Human chaperonin 10 is predominantly heptameric, although smaller oligomers were detected. These differences in structural assembly between species may explain differences in biological activity such as antigenicity.

Using C-terminal and N-terminal fragments, sequence 1–25 was identified as indispensable for aggregation. CD spectroscopy studies revealed that (i) a minimum at 202–204 nm correlates with aggregation and characterizes not only the spectrum of the mycobacterial protein, but also those of *E. coli* and human chaperonin 10 proteins; (ii) the interactions between subunits are of the hydrophobic type; and (iii) the anti-parallel *β*-pleated sheet is the main secondary structure element of subunits in both tetrameric and heptameric proteins.

The sequence-related chaperonin 10 (cpn10,[1] hsp10, or 10-kDa antigen) class of proteins assists the noncovalent assembly of other protein-containing structures *in vivo* (1). This biological activity requires aggregation of cpn10 into a heptameric structure (2). In addition to this activity, several cpn10 proteins such as the *Mycobacterium tuberculosis* and *Mycobacterium leprae* molecules are among the most potent stimulators of the immune system known (3–8). For example, in a leprosy patient, one in three T lymphocytes that respond to *M. leprae* may react to *M. leprae* cpn10 (4). Similarly, *M. tuberculosis* cpn10 induces T cell proliferation in healthy tuberculin reactors to an extent that is greater than that elicited by any other mycobacterial protein (5). Intriguingly, there is a dramatic difference in antigenicity between cpn10 proteins from different species: human cpn10 and *Escherichia coli* cpn10, for instance, are very poor immunogens (9).

In addition to antigenicity, chaperonins, at low concentrations, have other biological properties. For example, several micrograms or less of mycobacterial chaperonins/milliliter will immunize animals, stimulate T lymphocyte proliferation *in vitro*, and induce cytokine secretion from a human monocyte line and from human monocytes (3–8, 10, 11). They also induce apoptosis of human p19 cells.[2] Furthermore, there is evidence to suggest that human cpn10 may be involved in control over cell growth and development (9). These data indicate that cpn10 proteins have several distinct biological activities, namely as molecular chaperones and non-chaperone activities.

This study concerns the aggregation behavior of the *M. tuberculosis* cpn10 protein under a variety of different experimental conditions, in particular, low concentrations of cpn10 at which non-chaperone activities occur. Aggregation of both the full-length protein and truncated cpn10 peptides was examined. Furthermore, the secondary structure of the molecule was analyzed by CD spectroscopy. Most of the work was carried out using chemically synthesized full-length protein including the N-terminal and C-terminal fragments. Recombinant material was used for comparison.

Preliminary accounts on both the synthesis of the protein and its structure have been reported previously (13, 14). Here, we demonstrate that *M. tuberculosis* cpn10 exists, surprisingly, as a tetrameric aggregate with *β*-type structure in dilute solutions and in whole *M. tuberculosis* lysate. In the presence of a large molar excess of divalent ions, the protein has the expected heptameric structure and, together with cpn60, is functional in a refolding assay. In contrast, we show that *E. coli* cpn10 is heptameric under all conditions tested, while human cpn10 is predominately found as a heptamer, although dissociation into smaller oligomers takes place under certain solution conditions. These differences in structural assembly between species may help to explain differences in biological activity such as antigenicity.

MATERIALS AND METHODS

Chemical Synthesis of M. tuberculosis cpn10 and Fragments—The synthesis and purification of the *M. tuberculosis* protein and C-terminal and N-terminal fragments were performed by the solid-phase stepwise approach using *t*-butoxycarbonyl chemistry and according to a strategy

* The costs of publication of this article were defrayed in part by the payment of page charges. This article must therefore be hereby marked "*advertisement*" in accordance with 18 U.S.C. Section 1734 solely to indicate this fact.

¶ Present address: Max Planck Institute for Colloid and Interface Research, Colloid Chemistry Department, Kantstr. 55, D-14513 Telfow, FRG.

‖ To whom correspondence should be addressed. Tel.: 39-2-64433090; Fax: 39-2-66011579.

[1] The abbreviations used are: cpn10, chaperonin 10; HPLC, high performance liquid chromatography; SEC, size-exclusion chromatography; PBS, phosphate-buffered saline; AUC, analytical ultracentrifugation.

[2] G. Galli, P. Ghezzi, P. Mascagni, F. Marcucci, and M. Fratelli, submitted for publication.

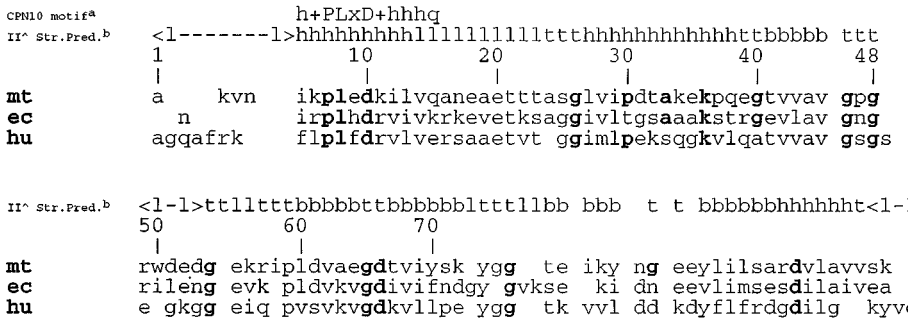

FIG. 1. **Alignment and secondary structure prediction of the *M. tuberculosis* (*mt*), *E. coli* (*ec*), and human (*hu*) cpn10 proteins discussed under "Results."** Numbering of residues refers to the *M. tuberculosis* protein. *Footnote a*, shown is the cpn10 motif described in the SWISS-PROT data base (release 30.0, October 1994). *h*, hydrophobic residues; *q*, mostly charged residues (Lys, Arg, Glu) or Gln. *Footnote b*, the secondary structure composition of cpn10 proteins was predicted by first aligning 27 sequences of cpn10 proteins and then considering the secondary structure of each section (separated by gaps) using two different algorithms: Chou-Fasman (12) and GORII (18). *II Str.Pred.*, secondary structure prediction; *h*, α-helix; *b*, β-strand; *t*, turn; *l*, loop. *Boldface* residues denote identity.

that uses chromatographic probes for the selective purification of synthetic proteins (15–17).[3] The details of this strategy applied to *M. tuberculosis* cpn10 and its fragments will be described elsewhere.[4] The material was, however, homogeneous by reversed-phase HPLC and had the correct M_r (peptide 1–99, 10,674; peptide 1–58, 6213; peptide 59–99, 4477; peptide 51–99, 5480; and peptide 26–99, 8007), sequence, and amino acid composition.

M. tuberculosis Lysate—Nonviable desiccated *M. tuberculosis* H37 RA (Difco) was used as source of naturally expressed *M. tuberculosis* cpn10. 200 mg of desiccated material was resuspended in 50 mM Tris, 150 mM KCl, 5 mM $MgSO_4$, 2.5 mM phenylmethylsulfonyl fluoride, 1 mM aprotinin, pH 7.4, and 50 mg of glass beads (150–210 μm; Sigma) were added. Protein extraction was performed by sonication of the suspension on ice (3 × 10 min, with a 1-min interval in between). After sonication, the suspension was centrifuged for 10 min at 13,000 rpm and 4 °C, and the supernatant was analyzed for protein content using the bicinchoninic acid protein assay (Pierce). An aliquot of the extract (corresponding to 70 μg of protein) was separated on a Superdex 75 SEC column using 50 mM Tris, 150 mM KCl, 1 mM $MgSO_4$ as a buffer, and fractions of 0.5 ml each were collected. Fractions of 100 μl each were coated on a 96-well microtiter plate (Nunc ImmunoPlate MaxiSorp), and detection of *M. tuberculosis* cpn10 was performed using a monoclonal antibody (SA12) specific for mycobacterial cpn10 (27) following standard enzyme-linked immunosorbent assay techniques.

Recombinant M. tuberculosis, E. coli, and Human cpn10 Proteins—*E. coli* cpn10 was purchased from Boehringer Mannheim and was used without further purification. Human cpn10 was expressed in *E. coli* and purified by reversed-phase HPLC as previously reported (19). *M. tuberculosis* was expressed either in baculovirus and purified by isoelectrofocusing in solution (20) or in *E. coli*. The details of expression in *E. coli* and purification will be described elsewhere. Briefly, for expression, the T7 expression system was used. Polymerase chain reaction amplification was performed using a pUC18 plasmid that contains the *M. tuberculosis* groESL-like operon as template. The resulting plasmid coding for *M. tuberculosis* cpn10 was transformed into BL21(DE3). Expression was carried out at 37 °C in M9ZB medium. Cells were harvested by centrifugation, resuspended in lysis buffer (50 mM Tris-HCl, 2 mM EDTA, pH 8.0), and centrifuged again. The pH of the supernatant was adjusted to 2.2 with trifluoroacetic acid, the suspension was centrifuged, and the resulting supernatant was applied directly to a semi-preparative reversed-phase HPLC column (Vydac C_{18}, 9 × 25 mm). The protein eluted at a concentration of acetonitrile N of ~40%. Fractions containing homogeneous material were pooled and lyophilized. The purity of the protein thus obtained was >95% as judged by both analytical HPLC and capillary electrophoresis. The entire expression and purification protocol yielded ~100 mg of pure (>95%) protein/liter of expression medium.

Size-exclusion Chromatography—Gel filtration experiments were conducted on a Superdex 75 column connected to a fast protein liquid chromatography instrument (Pharmacia) and a Jasco 875-UV detector. The column was calibrated using a mixture of globular standard proteins (Pharmacia Biotech low molecular weight gel filtration calibration kit) whose retention times were not affected by the different buffers used. Samples were eluted at 0.5 ml/min, and column effluent was monitored at both 280 and 214 nm.

Ultracentrifugation—A Beckman Optima XL-A analytical ultracentrifuge equipped with modern scanning absorption optics was used in all investigations. Sedimentation equilibrium experiments were performed at 20,000 and 30,000 rpm, scanning at 220, 230, and 280 nm and using the buffer as reference solvent at a temperature of 20 °C. For the experiments, six-channel 12-mm Kel-F (Beckman Instruments) "Yphantis cells" (21, 22) were used. The concentrations employed were 0.05, 0.2, and 1 mg/ml depending on the sample. The sedimentation equilibrium data were evaluated using the MSTARA program, which is described elsewhere (23). The solvent densities needed for the evaluation were determined at 20 °C using an Anton Paar Model DMA O2C precision density meter calibrated with CsCl solutions (24). For each density value, 10 consistent readings were obtained to minimize the experimental error. The partial specific volumes of the chaperones were calculated from their amino acid composition using the consensus formula given by Perkins (25).

CD Spectroscopy—CD measurements were performed on a Jasco J-600 spectropolarimeter calibrated with *d*-10-camphorsulfonic acid. Spectra, unless otherwise specified, were recorded in 0.1 M phosphate buffer at 22 °C in a cuvette with a 0.1-cm path length. Peptide and protein concentrations were kept at 0.1 mg/ml in all experiments. Spectra were the average of eight scans at 50 nm/min, each with a bandwidth set at 2 nm, and were base line-corrected by subtracting the corresponding blank. Although spectra were recorded in the 190–240 nm range, data below ~195 nm were not always reliable due to strong interferences of the solvent (0.1 M phosphate) at these wavelengths. The observed ellipticity was converted to mean residue weight ellipticity ($[\Theta]$/(degrees·cm^2·dmol^{-1})). Smoothing of the curves, using a mild function that increased the signal-to-noise ratio without altering the shape of spectra, was applied using the Jasco J-700 program. Superimposition of smoothed spectra with the raw curve was performed each time to check for artifacts.

pH titration experiments were performed by preparing a stock solution of peptide (2 mg/ml in either distilled water or slightly acidified water) and mixing aliquots of this solution with sufficient phosphate solution buffered at the pH of choice so as to yield a final solution containing 0.1 mg/ml peptide in 0.1 M phosphate. The exact pH was then monitored with a pH-meter equipped with a microelectrode. Prior to use, the final solution was equilibrated for 1 h at 22 °C in the CD chamber. During temperature studies, the cuvette containing the peptide solution and the CD chamber were equilibrated for 1 h prior to collection of data.

RESULTS

Fig. 1 shows the sequences of the three proteins considered in this work. Two of the *M. tuberculosis* cpn10 fragments (*i.e.* peptides 1–58 and 59–99) were selected because they include or exclude, respectively, a sequence (amino acids 46–59) predicted to be a loop region (Fig. 1). This loop contains the *M. tuberculosis* cpn10 monoclonal antibody (SA12)-binding site (5, 26, 27). SA12 is, within the cpn10 family, specific for the mycobacterial molecule. There were no special reasons for the

[3] H. L. Ball and P. Mascagni, submitted for publication.

[4] G. Fossati, G. Legname, P. Lucietto, H. L. Ball, P. Giuliani, A. R. Coates, and P. Mascagni, manuscript in preparation.

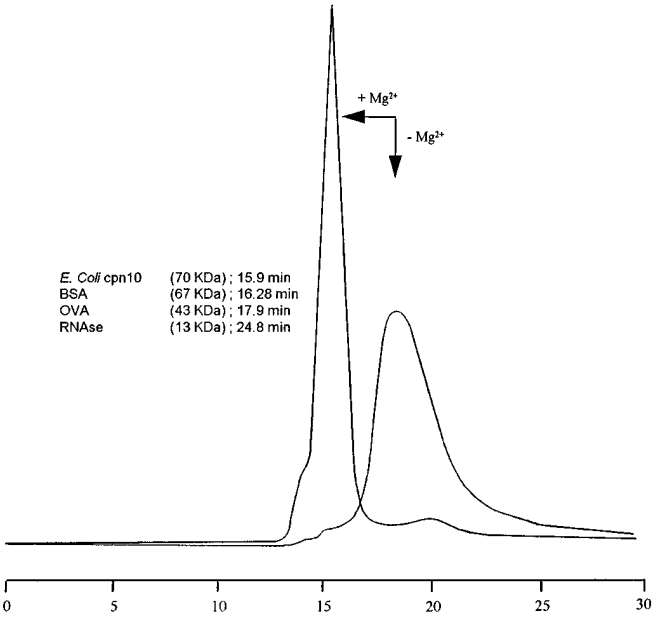

FIG. 2. **Size-exclusion chromatography of *M. tuberculosis* cpn10 (0.2 mg/ml) in PBS, pH 7.4, and in PBS plus 7 mM Mg^{2+}.** The addition of the latter changed the aggregation state of the protein from 4 to 7. *BSA*, bovine serum albumin; *OVA*, ovalbumin.

choice of the other two fragments other than the fact that peptide 51–99 cuts almost in the middle the loop antibody-binding region. This could provide information about which residues are necessary for antibody recognition. Peptide 26–99 begins with a conserved Gly, which follows a long sequence predicted to be another loop region (Fig. 1).

Chemical Synthesis

Preliminary accounts on the synthesis of *M. tuberculosis* cpn10 have been described previously (13, 14), while a complete account of the details will be reported elsewhere.[4] Here it should be noted that we have developed highly effective protocols for stepwise solid-phase synthesis of proteins and their purification. These protocols require (i) removal of deletion sequences by capping unreacted amino groups after each coupling step; (ii) addition of a chromatographic probe with enhanced lipophilic character to the last residue of the sequence; (iii) separation by reversed-phase HPLC of the probe-protein adduct from truncated sequences; and finally, (iv) removal of the probe by mild basic treatments (15–17).[3] The proteins thus recovered have a degree of purity generally >85%, as determined by a combination of mass spectrometry, HPLC, and capillary electrophoresis[3] and are further purified by either ion-exchange chromatography or isoelectrofocusing techniques.

The *M. tuberculosis* protein was synthesized and purified according to these protocols. The final purified product had the correct mass, amino acid composition, and sequence.[4] Furthermore, samples of recombinant material that became available during the final stages of this study were found to have the same physicochemical characteristics as synthetic *M. tuberculosis* protein.

Aggregation Studies

The synthetic protein and fragments were first analyzed by SEC for their ability to aggregate. In PBS, pH 7.4, the protein had an apparent molecular mass of ~40 kDa, which corresponded to an aggregation state of 4 (Fig. 2 and Table I). This was quite surprising since all cpn10 proteins reported to date have been described as heptamers. Indeed, samples of recombinant human and *E. coli* cpn10 proteins were found to be heptameric by the same technique (Table I). The synthetic origin of the protein was not responsible for this unexpected result since a sample of purified recombinant material had an identical SEC profile (Fig. 3). Furthermore, enzyme-linked immunosorbent assays using the *M. tuberculosis* cpn10-specific monoclonal antibody SA12 and SEC fractions of whole *Mycobacterium* lysate identified only one protein whose molecular mass corresponded to that of tetrameric cpn10 (Fig. 3).

The two larger fragments, *i.e.* peptides 26–99 and 51–99, also had retention times that, in a calibration curve, corresponded to an aggregation state of 4. A similar conclusion was reached when peptide 1–58 was tested, while peptide 59–99 eluted as either a trimer or dimer. The apparent molecular mass of the polypeptides did not change in the pH range 5–8.5, at which a calibration curve was still reliable using standard proteins (data not shown).

Given the unexpected nature of the oligomeric state of the protein, a second independent measurement of the aggregation properties of the cpn10 molecule was carried out by analytical ultracentrifugation (AUC). This confirmed that in PBS, pH 7.4, *M. tuberculosis* cpn10 was a tetramer (Table I). However, the fragments gave the following results. At concentrations varying between 0.05 and 1 mg/ml, peptide 1–58 was always a dimer, while all other C-terminal fragments were, in the same concentration range, monomeric (Table I). Given that, in some cases, the results from the two techniques (SEC and AUC) differed, and due to the superior reliability of AUC in the determination of the molecular mass, the values obtained from ultracentrifugation were taken as representative of the aggregation state of the polypeptides.

To explore the possibility that the *M. tuberculosis* cpn10 protein could adopt a heptameric form, a binding test was carried out with recombinant *E. coli* cpn60 (GroEL). Thus, it is well established that in order to exert its activity, the co-chaperone cpn10 protein must bind to cpn60 in the presence of Mg^{2+}/ATP (see, for example, Ref. 28). Furthermore, electron microscopy studies have shown that both proteins share a 7-fold axis of symmetry when in the complexed form (see, for example, Ref. 29). Indeed, *M. tuberculosis* cpn10 bound to GroEL, and the complex thus obtained was a functional one in a refolding assay.[4] These data suggest either that GroEL acts as a chaperone for the cpn10 protein by changing its aggregation state from 4 to 7 or that the smaller protein binds to GroEL in a tetrameric state. Alternatively, the transition between the two different aggregation states is due to the presence in the buffer of either ATP or Mg^{2+} ions or both. This hypothesis was verified by additional SEC experiments in the presence of Mg^{2+}/ATP. Magnesium ions alone were sufficient to change the aggregation state of cpn10 to 7 (Fig. 2 and Table I). Ultracentrifugation studies conducted under the same conditions confirmed this conclusion (Table I). A similar, although not quite so dramatic effect has been recently described for the cpn60 protein. Cross-linking of the native GroEL tetradecamer is accelerated by saturating amounts (10 mM) of Mg^{2+} ions (30).

Mg^{2+} could be substituted with Mn^{2+} and Ca^{2+} ions in inducing the change to heptamers, while monovalent ions, such as K^{+}, were ineffective (Table I). In the case of Zn^{2+} ions, a heptameric species and small amounts of larger aggregates were obtained (Table I). As to the shorter fragments, their aggregation states were not influenced by the addition of divalent ions, their retention times being the same in the presence or absence of Mg^{2+} (data not shown).

To evaluate whether parameters other than the divalent cations could influence the aggregation of the protein, additional SEC and AUC studies were carried out. Protein concen-

TABLE I
Summary of salient analytical ultracentrifugation and size-exclusion chromatography results on cpn10 proteins and M. tuberculosis cpn10 fragments

Peptide	Technique	Solvent[a]	Conc[b]	M_r[c] and aggregation state	
				pH 7.4	2.0 ≤ pH ≤ 3.4
E. coli cpn10	AUC	C	C_2	70,000 ± 5000 (n = 7)	
	SEC	D/D+Mg^{2+}/K^+	C_2	70,000 (n = 7)	
	SEC	A/A+Mg^{2+}	C_2	70,000 (n = 7)	
Human cpn10	SEC	A/A+Mg^{2+}	C_2	70,000 (n = 7)	
	SEC	D+K^+	C_2	Mainly 40,000 (n = 4)	
M. tuberculosis cpn10	AUC	C+Mg^{2+}	C_3	75,000 ± 5000 (n = 7)	
	AUC	A	C_2	47,000 ± 5000 (n = 4)	
	AUC	A	C_1	40,000 ± 10,000 (n = 4)	
	AUC	B	C_2		45,000 ± 5000 (n = 4)[d]
	SEC	D/A	C_2	40,000 (n = 4)	
	SEC	D+Mg^{2+}/Ca^{2+}/Mn^{2+}	C_2	70,000 (n = 7)	
	SEC	D+Zn^{2+}	C_2	70,000 (90%; n = 7) >100,000 (10%; n = NM)	
	SEC	A+Mg^{2+}	C_2	70,000 (n = 7)	
	SEC	C	C_3	70,000 (95%; n = 7) 40,000 (5%; n = 4)	
Peptide 59–99	AUC	A	C_2	5000 ± 1000 (n = 1)	
	AUC	A	C_1	5000 ± 1000 (n = 1)	
	AUC	B	C_2		6000 ± 2000 (n = 1)[e]
Peptide 51–99	AUC	C	C_3	3500 ± 1000 (n = 1)	
	AUC	C	C_2	3500 ± 1000 (n = 1)	10,000 ± 500 (n = 2)[f]
Peptide 26–99	AUC	C	C_3	5000[g] (n = 1)	
	AUC	C	C_2	7000 ± 3000 (n = 1)	17,000 ± 1000 (n = 2)[f]
Peptide 1–58	AUC	C	C_3	10,000 ± 1000 (n = 2)	
	AUC	A	C_2	10,000 ± 2000 (n = 2)	
	AUC	A	C_1	9500 ± 2000 (n = 2)	

[a] A = PBS; B = 0.01 M phosphate; C = 0.1 M phosphate; D = 0.1 M Tris.
[b] C_1 = 0.05 mg/ml; C_2 = 0.2 mg/ml; C_3 = 1 mg/ml. Ions such as Mg^{2+}, Ca^{2+}, Mn^{2+}, Zn^{2+}, and K^+ were added to the buffer of choice to a final concentration of 7 mM.
[c] In the case of SEC the M_r was obtained from calibration curves and is approximated to the nearest thousand. n is the number of subunits contained in the aggregate.
[d] pH 2.0.
[e] pH 3.0.
[f] pH 3.4.
[g] Noisy data; it was not possible to calculate the error.

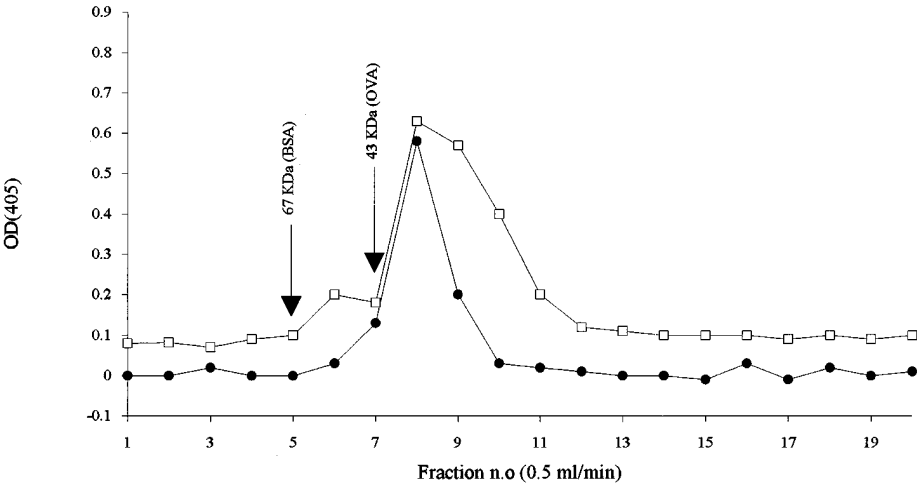

FIG. 3. **Enzyme-linked immunosorbent assays on size-exclusion chromatography fractions of recombinant *M. tuberculosis* cpn10 (●) and *M. tuberculosis* lysate (□).** Fractions (0.5 ml) were collected every minute after 13 min from injection. 100 μl of each fraction were coated on a 96-well microtiter plate, and the presence of *M. tuberculosis* cpn10 was revealed with the *M. tuberculosis* cpn10 monoclonal antibody SA12 using standard enzyme-linked immunosorbent assay techniques. *BSA*, bovine serum albumin; *OVA*, ovalbumin.

tration and type of buffer were examined. Also, solution pH was studied (by ultracentrifugation only) because the CD results (see below) indicated that both the protein and its C-terminal fragments undergo a conformational change at acidic pH values.

When the protein concentration was kept between 0.1 and 0.2 mg/ml, an aggregation state of 4 was found irrespective of the buffer used (*i.e.* 0.1 mM Tris with or without 10 mM KCl and PBS without Mg^{2+}/Ca^{2+}) (Table I). The addition of Mg^{2+} converted the protein to a heptamer in all of these solvents. When the concentration of the protein was increased to 1 mg/ml and the solvent was 0.1 M phosphate, the heptamer was the most abundant species in solution (~95%) even in the absence of Mg^{2+}. Interestingly, lowering the phosphate concentration to

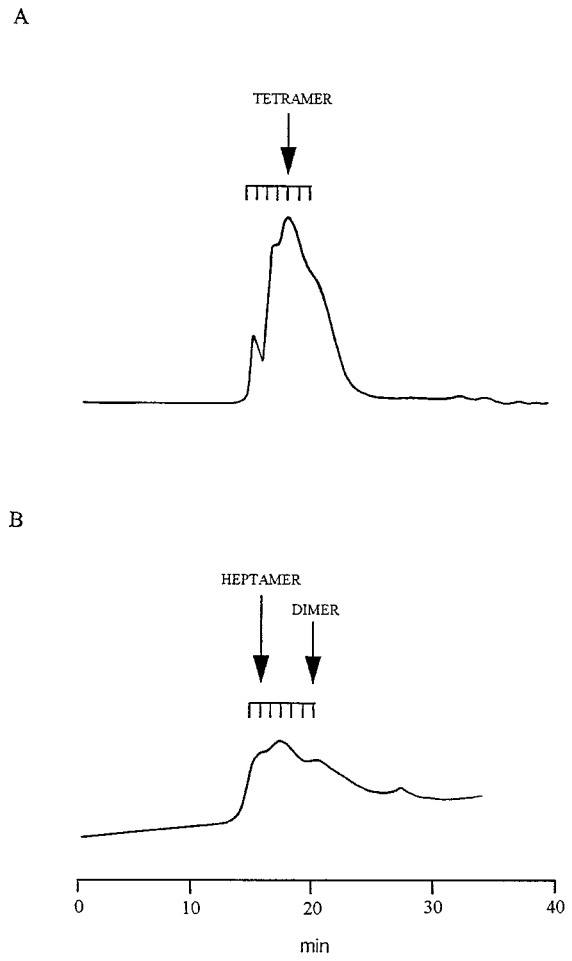

FIG. 4. **Size-exclusion chromatography of *M. tuberculosis* cpn10 (1 mg/ml) in PBS, pH 7.4 (*top trace*), and human cpn10 (0.2 mg/ml) in 0.1 M Tris buffer, pH 7.4 (*bottom trace*), illustrating the presence of different oligomeric structures.**

that of PBS (*i.e.* ~10 mM) while maintaining the protein concentration at 1 mg/ml gave aggregation species that ranged from that of a heptamer to either a dimer or trimer (Fig. 4*A* and Table I). Finally, at acidic pH and in 10 mM phosphate buffer, the protein was still a tetramer (Table I).

Similar studies conducted on recombinant *E. coli* cpn10 (also known as GroES) showed that the protein existed in solution only as a heptamer (Table I). Human cpn10 had instead a behavior intermediate between that of GroES and that of *M. tuberculosis* cpn10 since it was heptameric in all cases tested, except in a 0.1 M Tris solution, pH 7.4, where it was a mixture of various aggregation states (Fig. 4*B*), and in the same solution plus 10 mM KCl, where it was mainly tetrameric (Table I). Finally, peptides 26–99 and 51–99, which were not influenced by all the parameters discussed above (data not shown), became dimers at pH 3.4, while peptide 59–99 was still monomeric at a similar pH (Table I).

CD Spectroscopy

The fragments and the *M. tuberculosis* cpn10 protein (0.1 mg/ml) were initially studied in phosphate buffer (0.1 M) at neutral pH (Fig. 5*A*). With the exception of peptide 59–99, which had minima at about 215 and 202 nm, the other molecules had either an intense band at 198 nm and a shoulder at ~220 nm (peptides 51–99 and 26–99) or a minimum at 203 nm and shoulders at about 198 and 217 nm (full-length protein). Furthermore, the intensities of the spectra decreased on going from peptide 51–99 to protein. Peptide 1–58, in addition to the intense band at 198 nm, had a shoulder between 225 and 230 nm (Fig. 5*A*). A more detailed study on the CD structure of these peptides was then carried out, beginning with the shortest sequence.

Peptide 59–99—The CD spectrum of this peptide was the only one of those shown in Fig. 5*A* with an apparently more defined secondary structure composition. CD spectra with minima between 215 and 220 nm have been attributed to proteins with a high content of anti-parallel β-sheet and a nonsecondary structure contribution from aromatic residues (this peptide contains four tyrosines) (31).

pH titration experiments led to a decrease of the contribution at 202 nm and an increase in the minimum at 215 nm (Fig. 5*B*). At pH 3.0, where the peptide had a stable structure (32) and was monomeric, there was only the band at 215 nm.

Peptide 51–99—The addition of only eight residues to peptide 59–99 dramatically affected the CD spectrum of the resulting 51–99 molecule. Thus, although a β-sheet contribution could still be deduced from the shoulder at 220 nm, the main CD band was at 198 nm (Fig. 5, *A* and *C*). Changing the solution pH led to a blue shift of the former to 217 nm and an increase in its intensity, which became maximal at pH 3.5. At this pH, a minimum at 204 nm replaced that at 198 nm (Fig. 5*C*). Notice that the presence of the latter could not be excluded since the 204 nm band was very broad. Under these conditions of solvent composition and pH, the peptide was a dimer (see above and Table I).

Peptide 26–99—A trend similar to that found for peptide 51–99 applied to peptide 26–99, which was monomeric and dimeric at neutral and acidic pH, respectively. Thus, the broad and intense signal centered at 198 nm in the spectrum at pH 7.4 moved, at pH 3.4, to ~203 nm, while the shoulder at 220 nm became more intense and shifted to 215 nm (Fig. 5*D*). An isosbestic point at 209.5 nm, essentially in the same position as that of peptide 59–99, characterized the pH titration experiment.

Peptide 1–58—Unlike the other fragments, the region of the protein corresponding to its N-terminal half was dimeric at neutral pH and at a wide range of peptide concentrations (*i.e.* 0.05–1 mg/ml) (Table I). The spectrum at pH 7.4 had an intense band at 198 nm and a shoulder between 225 and 230 nm (Fig. 5*A*) and did not change upon varying the solution pH (data not shown).

Peptide 1–99—As discussed above, the *M. tuberculosis* protein adopts, in the absence of divalent cations, a tetrameric structure unseen in the case of other members of this class of proteins. CD studies were therefore conducted not only as a function of the solution pH, but also in the presence of Mg^{2+} and as a function of temperature and solvent composition.

The spectrum of the *M. tuberculosis* protein (Fig. 5*A*) was qualitatively similar to those of *E. coli* cpn10, synthetic rat cpn10 (14), and recombinant human cpn10. In particular, the *E. coli* protein had a minimum at 202 nm and a shoulder at 197 nm, while human cpn10 (and rat cpn10; the two proteins differ by one residue) had minima at 203 and 197 nm (Fig. 6). Thus, the band at 202–203 nm and the shoulder at 197–198 nm are characteristic of this class of proteins and independent of their origin or aggregation state.

The intensity of the 204 nm band was, however, larger in the case of mammalian and *E. coli* proteins. The aggregation state was only partly responsible for these changes since the spectrum of the *M. tuberculosis* protein in its heptameric state (*i.e.* in the presence of Mg^{2+}; see below) was still less intense than those of the other two chaperonins. Possible explanations for this difference could be either the presence in solution of small

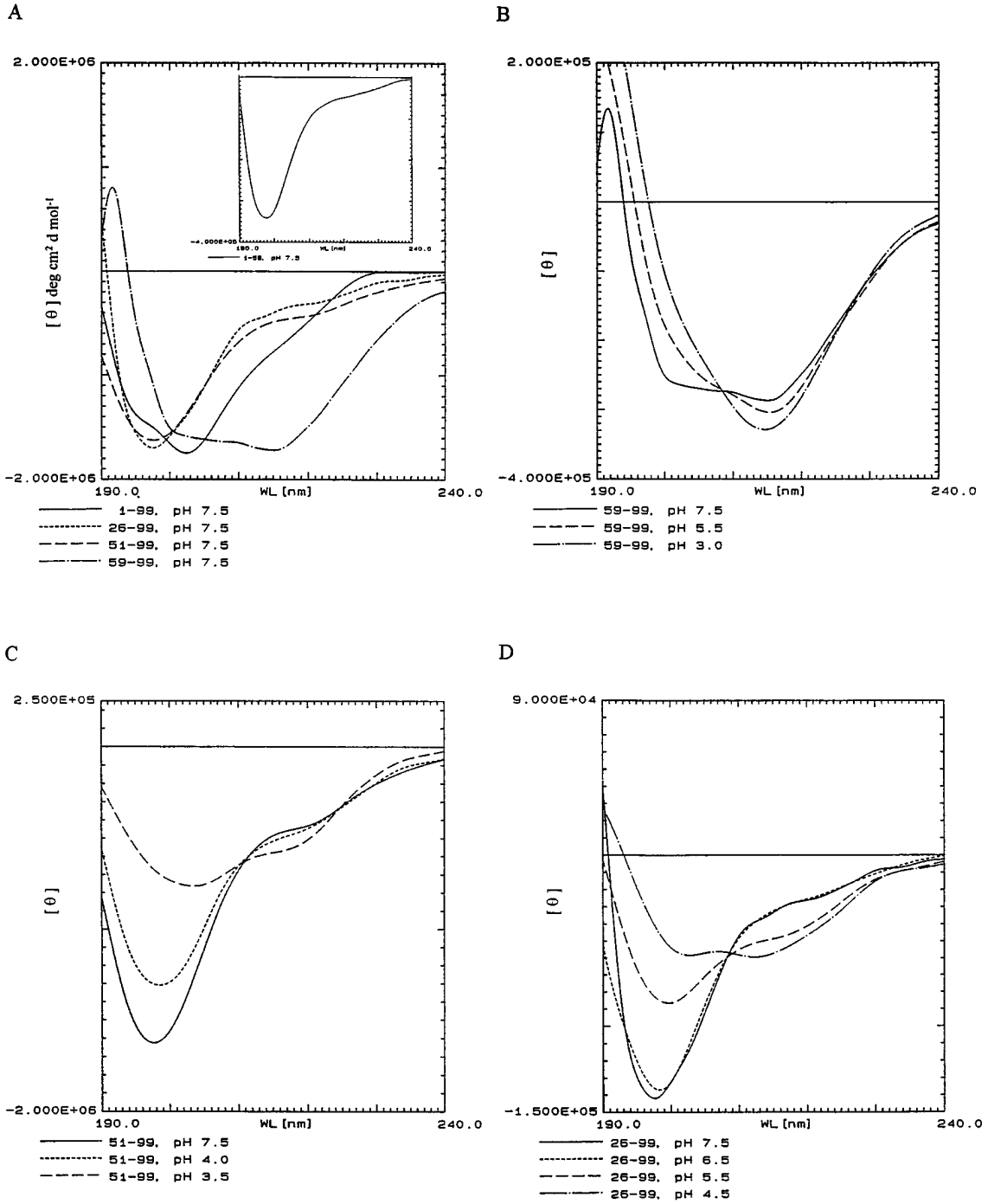

FIG. 5. **CD spectra of *M. tuberculosis* cpn10 and fragments.** *A*, *M. tuberculosis* cpn10 and C-terminal fragments (0.1 mg/ml) in 0.1 M phosphate buffer, pH 7.4. The spectrum of peptide 1–58 is shown in the *inset*. The spectra of the C-terminal fragments had different intensities (see "Results," the other panels of this figure, and Fig. 7). Therefore, to enable their visual comparison, the spectra of peptides 59–99 and 26–99 and the full-length protein were multiplied by factors of 6, 12, and 300, respectively. *B*, CD curves of peptide 59–99 at different pH values. All fragments and the full-length protein were scarcely soluble in the approximate pH range 4–5.5. Spectra at these pH values were therefore not obtained. *C*, as in *B*, but for peptide 51–99. *D*, as in *B* and *C*, but for peptide 26–99. *WL*, wavelength.

concentrations of tetrameric *M. tuberculosis* cpn10 or a difference balance, in the three proteins, of the residues/regions contributing to the 204 nm band and the less intense 198 nm band.

Lowering the pH of *M. tuberculosis* cpn10-containing solutions induced a shift to 204 nm of the broad signal at 203 nm similar to that seen for the C-terminal fragments, while the shoulder at 217 nm became more pronounced (Fig. 7*A*). An isosbestic point at 210.5 nm, together with invariance of the spectral features between pH 4.5 and 2 (spectra in this pH range were essentially identical; data not shown), indicated the existence of an equilibrium between at least two species, one (or more) at pH 7.4 and a second conformation stable in the pH 4.5 to 2 interval.

Qualitatively, the addition of Mg^{2+}, which aggregation studies had shown to induce a transition from tetramers to heptamers, led to the same changes (*i.e.* shift of the 203 nm band to 204 nm and increase in the intensity of the 217 nm shoulder) observed during pH titration (Fig. 7*B*). In particular, virtually no changes were observed when 1 or <1 eq ($C_{Mg^{2+}} \leq \sim 0.01$ mM)

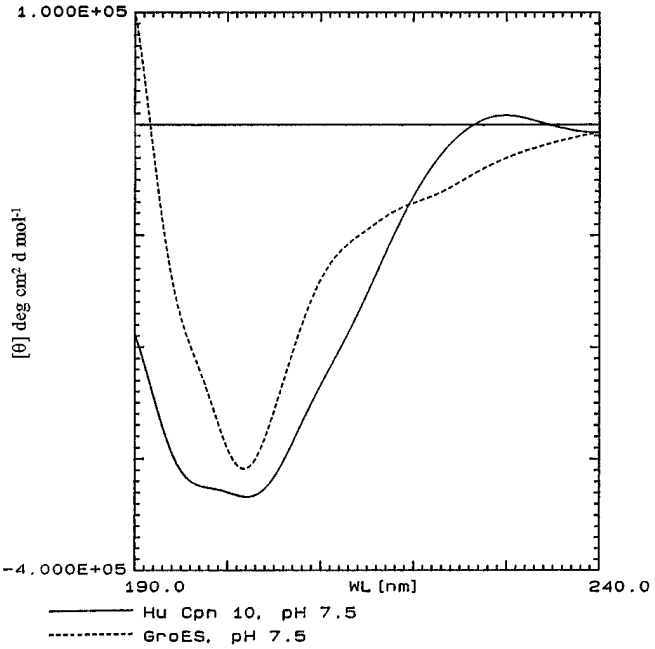

FIG. 6. **CD spectra of *E. coli* and human (*Hu*) cpn10 proteins (0.1 mg/ml) in 0.1 M phosphate buffer, pH 7.4. *WL*, wavelength.**

of magnesium ions/protein subunit was added, while a continuous change in the shape of the spectrum was obtained upon adding 5 eq of Mg^{2+} (0.05 mM) and up to a total magnesium concentration of ~5 mM. These results suggested that there was no stoichiometric binding of the ion to the cpn10 protein.

Modulation of the intensities of the minima at ~200 nm also occurred during temperature studies. Thus, at 0 °C, the spectrum had two almost equally intense bands, at 199 and 203 nm, respectively, while raising the temperature to 30 °C led to a sharpening of the latter, which moved to 204 nm. At this temperature, the 198 nm contribution was reduced considerably (Fig. 7*C*).

Finally, the addition of MeOH to aqueous solutions of *M. tuberculosis* cpn10 led to a CD spectrum resembling that of an all-β-structure (Fig. 7*D*) (31). This suggested that the ability to form anti-parallel β-strands shown by the C-terminal fragments was maintained in the full-length protein.

DISCUSSION

The work that we describe here provides, for the first time, CD data on the secondary structure of *M. tuberculosis* cpn10, leads to a hypothesis for the tertiary structure, and demonstrates, surprisingly, that the main quaternary unit is a tetramer. The following is a detailed discussion of the main findings.

Aggregation—cpn10 proteins are known to assemble into heptameric structures and, in the presence of Mg^{2+}/ATP, form a complex with cpn60 tetradecamers that functions as a molecular chaperone. Electron microscopy studies have shown that both cpn10 and cpn60 share a 7-fold axis of symmetry in the complexed form (see, for example, Ref. 29). Prior to the present work, these structures were reported to be quite stable (33). The results of SEC and AUC that we reported here confirm that *E. coli* and human cpn10 heptamers are stable under a wide variety of conditions, but, surprisingly, *M. tuberculosis* cpn10 is predominantly a tetramer under most of the conditions tested. Heptameric species were also obtained and shown to prevail in the presence of a large molar excess of divalent ions (*e.g.* Mg^{2+}, phosphate, etc.). The role of the latter does not seem to involve secondary structure changes deriving from an increase in the solution ionic strength since replacing magnesium with potassium did not lead to heptamerization. A possible explanation for these observations is that divalent ions bring the surfaces of neighboring subunits into closer contact with one another.

The heptameric structure of *M. tuberculosis* cpn10 acts as a molecular chaperone by binding to *E. coli* cpn60 and generating a complex functional in a refolding assay. This shows that both *M. tuberculosis* cpn10 and *E. coli* cpn10 associate in the same way, *i.e.* as heptamers with the cpn60 tetradecamer.

What is the significance of tetrameric *M. tuberculosis* cpn10? The first clue comes from the our observation that *M. tuberculosis* cpn10 is tetrameric in low protein and low divalent ionic solutions. This suggests that, in nature, where a wide variety of conditions are present, the tetrameric form may predominate. Indeed, this appears to be the case since *M. tuberculosis* lysate has only one species that binds to anti-cpn10 monoclonal antibody and has the molecular mass of a tetramer. (It is important to note that the monoclonal antibody used in this experiment binds to both tetrameric and heptameric forms of *M. tuberculosis* chaperonin,[5] ruling out the existence of heptameric species in mycobacterial lysate.)

Is *M. tuberculosis* cpn10 biologically different from *E. coli* or mammalian cpn10? The most obvious difference is immunogenicity. For example, *M. tuberculosis* cpn10 is highly antigenic (3–7) while *E. coli* and mammalian cpn10 proteins are not (9). Furthermore, recent data suggest that *M. tuberculosis* cpn10 can stimulate monocytes (10), macrophages (11), and synovial fibroblast-like cells.[6] In contrast, human and *E. coli* cpn10 proteins are poor immunogens (9). It is very difficult even to raise low affinity antibodies against human cpn10 by repeated injections into animals (9). Thus, the different behavior toward aggregation shown by the cpn10 proteins described in this work and, in particular, the ability of the *M. tuberculosis* homologue to form stable tetrameric species may explain the different biological activities of cpn10 proteins.

The data on aggregation using the protein's fragments suggest where, in the sequence, the regions involved in subunit interactions are approximately located. Thus, the behavior of peptides 1–58 and 26–99 and the full-length protein clearly indicates that sequence 1–25 is pivotal to aggregation to tetramers/heptamers. Interestingly, the motif h+PL*x*D + hhhq, which spans residues 6–15, has been proposed as the cpn10 protein fingerprint (Fig. 1). Here, it is proposed that this sequence is one of the regions required for tetramer/heptamer formation. Another aggregation region may be in the C-terminal half of the protein, although the data are not sufficient for a more precise and unequivocal location.

Secondary Structure—Central to this discussion are the minima at 198 and 203–204 nm. The first has been traditionally attributed to the random coil structure. Spectra with similar characteristics are also of proteins (*e.g.* soybean trypsin inhibitor (34)) whose crystal structure data show to be made of anti-parallel pleated sheets that either are very much distorted or contain very short irregular strands (34, 35).

Here, a β-contribution seemed likely due to the structure of peptide 59–99, which, at low pH, was assigned to a β-sheet, and the existence in the spectra of all other polypeptides of minima/shoulders at 215–220 nm. Furthermore, the spectrum of *M. tuberculosis* cpn10 in water/MeOH mixtures was that of proteins with a high β-pleated sheet content. The shoulder between 225 and 230 nm seen in the spectrum of peptide 1–58 could also be interpreted as deriving from β-sheets since pro-

[5] G. Fossati, unpublished observation.
[6] F. Marelli, P. Mascagni, and A. R. Coates, unpublished observation.

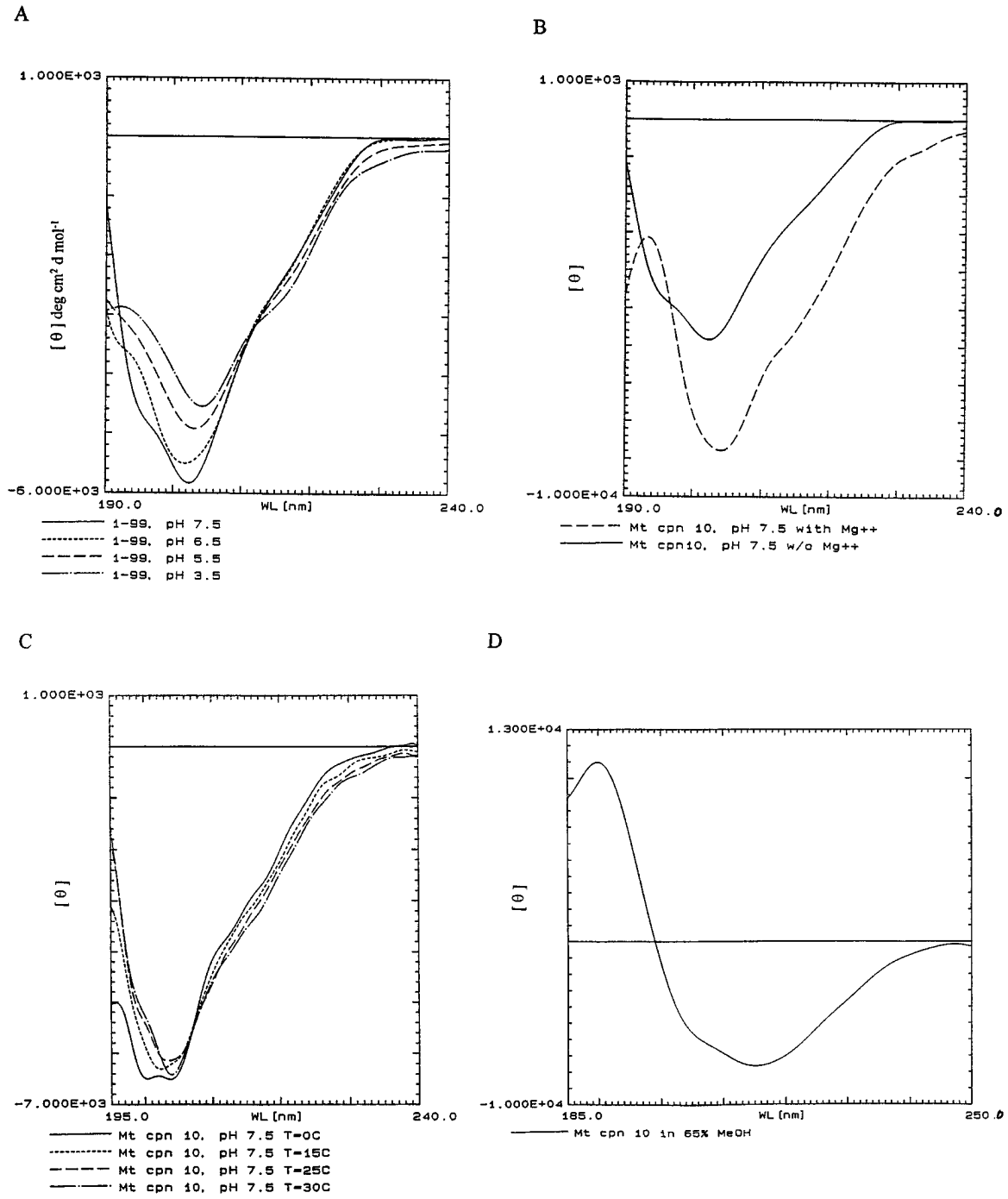

FIG. 7. **CD spectra of *M. tuberculosis* (*Mt*) cpn10 (0.1 mg/ml) in 0.1 M phosphate buffer.** *A*, the protein at different pH values; *B*, spectra recorded in the absence and presence of Mg^{2+} (7 mM); *C*, temperature studies carried out between 0 and 30 °C; *D*, protein in a 0.1 M phosphate/MeOH (35:65) mixture. *WL*, wavelength.

teins with this fold and scarce aromatic contribution exhibit a minimum in this region of the spectrum (31). A contribution of the random coil type to the structure of the protein and fragments was also probable since the H-α chemical shift of residues contained in sequence 17–32 of GroES (sequence 19–34 in *M. tuberculosis* cpn10) has been shown to be virtually identical to those reported for random coil peptides (36).

The minimum at 203–204 was more difficult to interpret. Its assignment to an α-helix seemed unlikely due to the lack of the intense band at 222 nm. On the other hand, the spectra of both polyproline II (37) and type I β-turns (Woody's class C spectrum) (38) have minima in this wavelength range.

A more positive assignment derived from the observation that the main band of monomeric peptides 51–99 and 26–99 is at 198 nm while the minimum at 203–204 nm and the shoulder at 215–217 nm characterize the spectra of dimeric peptides 51–99 and 26–99 and tetrameric and heptameric cpn10 proteins. Thus, based on these observations, it was concluded that the 203–204 nm band correlates with aggregation, whereas the opposite applies to the minimum at 198 nm. Whether these changes in quaternary structure are accompanied by changes in secondary structure (for instance, random coil to polyproline II-like structure) of parts of the molecule or whether the 203–204 nm contribution derives directly from the interactions between subunits cannot be concluded on the basis of these data only.

Changes in the intensities of the 198 and 203–204 nm minima were also observed during the temperature studies of the full-length protein. In particular, the band at 198 nm became more intense at 0 °C and vanished almost completely at 30 °C, where it was replaced by the 204 nm minimum. Since we had correlated similar changes in secondary structure with changes in the aggregation state and due to the fact that hydrophobic interactions are weaker at low temperature (39), we conclude that the oligomeric structure of the protein is stabilized by hydrophobic interactions.

Conclusions—The results presented here indicate that for the *M. tuberculosis* cpn10 protein, an equilibrium exists in solution between mainly tetrameric and heptameric forms, which can be modulated by the protein concentration, the addition of divalent cations, or the concentration of the phosphate ion. Monomeric protein was never clearly detected. However, the need to explain transition from tetramers to heptamers requires either the presence in solution of small amounts of monomer or dissociation of tetramers into at least one monomeric species and then reassembly into the larger oligomer. Comparison of the aggregation behavior of the N-terminal and C-terminal fragments with that of the full-length protein led to the proposal of sequence 6–15 as one of the protein aggregation motifs. This conclusion is in agreement with recent data that indicate that in rat cpn10, the first 1–25 residues are essential for heptamerization (17).

CD results were consistent with the existence of aggregation equilibria. The latter could be followed by monitoring the intensity of the minima at 198 and 203–204 nm. The CD data also permitted us to conclude that the protein adopts a mainly anti-parallel β-fold consisting of two different regions, each containing an anti-parallel β-sheet: the first region comprises residues 1–45, and the second comprises either peptide 55–99 or 59–99, with peptide 46–54 (46–58) forming a large loop connecting the two sheets. The reasons for these assumptions were (i) our data that indicate that peptide 59–99 has a spectroscopic and aggregation behavior different from that of the other fragments; (ii) the assignment of peptide 46–58 to a loop region containing the protein antibody-binding site (5, 27); (iii) the ability of the protein to adopt a mainly β-fold, as shown by its CD spectrum in water/MeOH mixtures; and (iv) the recently published indication that the nearly complete crystal structure of GroES is made of identical subunits with a mainly β-barrel fold (40). β-Barrels are generally formed by two β-sheets that are joined together and packed against each other.

CD data were also used to conclude that the secondary structure composition of subunits is similar in both stabilized tetramers (*i.e.* the CD structure at acidic pH values) and heptamers and that contact between subunits is mainly through hydrophobic forces. Finally, the spectra of *E. coli* and human cpn10 molecules were also characterized by minima at 198 and 202–204 nm. Thus, the latter, which was found to correlate with aggregation, appears to be a general feature of cpn10 molecules.

REFERENCES

1. Ellis, R. J., and Van der Vies, S. M. (1991) *Annu. Rev. Biochem.* **60,** 321–347
2. Saibil, H., Dong, Z., Wood, S., and Auf Der Mauer, A. (1991) *Nature* **353,** 25–26
3. Coates, A. R. M. (1995) in *The Chaperonins* (Ellis, R. J., ed) Academic Press Ltd., London, in press
4. Mehra, V., Bloom, B. R., Bajardi, A. C., Grisso, C. L., Sieling, P. A., Alland, D., Convit, J., Fan, X., Hunter, S. W., Brennan, P. J., Rea, T. H., and Modlin, R. L. (1992) *J. Exp. Med.* **175,** 275–284
5. Barnes, P. F., Mehra, V., Rivoire, B., Fong, S. J., Brennan, P. J., Voegtline, M. S., Minden, P., Houghten, R. A., Bloom, B. R., and Modlin, R. L. (1992) *J. Immunol.* **148,** 1835–1840
6. De Bruyn, J., Bosmans, R., Turneer, M., Weckx, M., Nyabenda, J., Van Vooren, J. P., Falmagne, P., Wiker, H. G., and Harboe, M. (1987) *Infect. Immun.* **5,** 245–252
7. Oftung, F., Mustafa, A. S., Husson, R., Young, R. A., and Godal, T. (1987) *J. Immunol.* **138,** 927–931
8. Orme, I. M. (1988) *J. Immunol.* **140,** 3589–3593
9. Cavanagh, A. C., and Morton, H. (1994) *Eur. J. Biochem.* **222,** 551–560
10. Friedland, J. S., Shattock, R., Remick, D. G, and Griffin, G. E. (1993) *Clin. Exp. Immunol.* **91,** 58–62
11. Petermans, W. E., Raats, L. J., Langermans, J. A., and van Furth, R. (1994) *Scan. J. Immunol.* **39,** 613–617
12. Chou, P. Y., and Fasman, G. D. (1974) *Biochemistry* **13,** 222–245
13. Fossati, G., Lucietto, P., Giuliani, P., Ball, H. L., Chan, A. W. E., Leoni, F., Gromo, G., Coates, A. R. M., and Mascagni, P. (1993) in *Proceedings of the Second Japanese Symposium on Peptide Chemistry* (Yanaihara, N., ed) pp. 235–238, ESCOM Science Publishers B. V., Leiden, The Netherlands
14. Mascagni, P., Chan, A. W. E., Coates, A. R. M., Fossati, G., Giuliani, P., and Lucietto, P. (1994) in *Proceedings of the Thirteenth American Peptide Symposium* (Hodges, R. S., and Smith, J. A., eds) pp. 763–765, ESCOM Science Publishers B. V., Leiden, The Netherlands
15. Ball, H. L., and Mascagni, P. (1992) *Int. J. Pept. Protein Res.* **40,** 370–379
16. Ball, H. L., Bertolini, G., Levi, S., and Mascagni, P. (1994) *J. Chromatogr.* **686,** 73–83
17. Ball, H. L., Giuliani, P., Lucietto, P., Fossati, G., and Mascagni, P. (1995) *Biochem. Pept. Proteins Nucleic Acids* **1,** 39–44
18. Garnier, J., Osguthorpe, D. J., and Robson, B. (1978) *J. Mol. Biol.* **120,** 97–120
19. Legname, G., Fossati, G., Gromo, G., Monzini, N., Marcucci, F., and Modena, D. (1995) *FEBS Lett.* **361,** 211–214
20. Atkins, D., Al-Ghusein, H., Prehaud, C., and Coates, A. R. M. (1994) *Gene* (*Amst.*) **150,** 145–148
21. Yphantis, D. A. (1964) *Biochemistry* **3,** 297–317
22. Teller, D. C. (1973) *Methods Enzymol.* **27,** 346–441
23. Harding, S. E., Horton, J. C., and Morgan P. J. (1992) in *Analytical Ultracentrifugation in Biochemistry and Polymer Science* (Harding, S. E., Rowe, A. J., and Horton, J. C., eds) Royal Society of Chemistry, Cambridge
24. Kratky, O., Leopold, H., and Stabinger, H. (1973) *Methods Enzymol.* **27,** 98–110
25. Perkins, S. J. (1986) *Eur. J. Biochem.* **57,** 169–173
26. Minden, P., Houghten, R. A., Spear, J. R., and Shinnick, T. M. (1986) *Infect. Immun.* **53,** 560–564
27. Verbon, A., Hartskeerl, R. A., and Kolk, A. H. J. (1991) *Clin. Exp. Immunol.* **86,** 6–12
28. Goloubinoff, P., Christeller, J. T., Gatenby, A. A., and Lorimer, G. H. (1989) *Nature* **342,** 884–889
29. Saibil, H., and Wood, S. (1993) *Curr. Biol.* **3,** 207–213
30. Azem, A., Diamant, S., and Goloubinoff, P. (1994) *Biochemistry* **33,** 6671–6675
31. Perczel, A., Park, K., and Fasman, G. D. (1992) *Proteins Struct. Funct. Genet.* **13,** 57–69
32. Chan, E., Fossati, G., Giuliani, P., Lucietto, P., Zaliani, A., Coates, A. R. M., and Mascagni, P. (1995) *Biochem. Biophys. Res. Commun.* **211,** 14–20
33. Ellis, R. J. (1990) *Science* **250,** 954–959
34. Richardson, J. S. (1981) *Adv. Protein Chem.* **34,** 167–339, and references therein
35. Manavalan, P., and Johnson, W. C., Jr. (1983) *Nature* **305,** 831–832
36. Landry, S. J., Zeilstra-Ryalls, J., Fayet, O., Georgopoulos, C., and Gierasch, L. M. (1993) *Nature* **364,** 255–258
37. Woody, R. W. (1992) *Adv. Biophys. Chem.* **2,** 37–79
38. Woody, R. W. (1985) in *The Peptides* (Hruby, V. J., ed) Vol. 7, pp. 15–115, Academic Press, New York
39. Pratt, L. R., and Chandler, D. (1977) *J. Chem. Phys.* **67,** 3683–3695
40. Saibil, H. R. (1994) *Nature Struct. Biol.* **1,** 838–842